Journal of Fluids and Structures (1997) **11,** 271–291

NUMERICAL STUDY OF THE INSTABILITIES IN THE NEAR WAKE OF A CIRCULAR CYLINDER AT LOW REYNOLDS NUMBER

J. H. GERRARD

Manchester School of Engineering, University of Manchester
Manchester M13 9 PL, U.K.

(Received 8 March 1996 and in revised form 16 August 1996)

In experiments it was found by Al-Khafaji that the normally steady wake at Reynolds number 29 (Re based on diameter d) could be made to oscillate by the inclusion of a small diameter ($d/8$) control rod at certain positions on the centreline of the near wake. Following this work an existing Navier–Stokes solver was applied to the same problem. The control rod was modelled by inserting a vortex pair at a fixed point on the wake axis at each side of this point. The vortices diffuse as they are convected downstream. An asymmetry developed in the vortex pair and an oscillating wake was found for a range of positions on wake axis. The instability was investigated by observing the onset and exponential growth of oscillations in the asymmetry of the velocity field, the vorticity and the cylinder lift coefficient. Results are presented which show that the driving force at $\mathrm{Re} < \mathrm{Re_c}$ is the asymmetry in the near wake which convects downstream. Interaction with the control rod produces oscillations at the rod which feed back to the cylinder to initiate the exponential growth of C_L. At $\mathrm{Re} > \mathrm{Re_c}$ the exponential growth of C_L takes place without a control in the wake. The growth rate, the frequency and C_L as functions of Re are determined and compared with other work.

1. INTRODUCTION

DESPITE THE IMMENSE LITERATURE on cylinder wake flows, publications in recent years have been on the increase. This is not only because of practical interest in separated flows and control mechanisms; much interest also stems from concern about stability of the flows and transition to turbulence. Many studies in the past which were aimed at the fundamental description of the near wake of the cylinder are now found to be of significance as far as wake instability is concerned. We may mention, for example, the finding of Coutanceau & Bouard (1977) that for $14 < \mathrm{Re} < 40$ a back flow velocity, distributed similarly through this range, reaches a value of $0{\cdot}08U$(U = freestream speed) at the Re at which wake oscillations start. Taneda (1963) and Nishioka & Sato (1978) found that transverse cylinder oscillations produce wake oscillations which convect downstream, and that for $\mathrm{Re} > 20$ the oscillation grew exponentially in the downstream direction. The critical value of $\mathrm{Re_c}$, the Re at which wake oscillation starts, is increased by the effect of confining walls. Shair *et al.* (1963) found that $\mathrm{Re_c}$ could be increased to 135 by confinement up to 20%. Koch (1985) showed the effect of blockage ratio on his stability analysis. By varying the side wall distance from a symmetric wake flow, a bifurcation point was discovered: this was absent without interference from the side walls. Following the work of Leal & Acrivos (1969) and Wood (1963), Bearman

0889–9746/97/030271 + 21 $25.00/fl960077

TABLE 1

Experimental results of the critical gap between an interference element and the back of a circular cylinder for the suppression of vortex shedding

Source	Re Range	Gap size g/a	Plate length L_p/d	Interference element	Test rig
Roshko (1954)	14 500	5·4	1·14	Splitter plate	Wind tunnel
Gerrard (1978)	150	5·4	1	Splitter plate	Water tank
Grove *et al.* (1964)	25–300	5·0	1–4	Splitter plate	Oil tunnel
Unal & Rockwell (1988)	140–5000	4·6	24	Splitter plate	Water tunnel
Thomas & Kravs (1964)	62–500	5·2	—	Circular cylinder	Wind tunnel
Ishigai *et al.* (1972)	8×10^3	5·6	—	Circular cylinder	Wind tunnel
Zdravkovich (1977)	$8{\cdot}3 \times 10^4$	5·0	—	Circular cylinder	Wind tunnel
Zdravkovich & Stanhope (1972)	1×10^5	5·0	—	Circular cylinder	Wind tunnel

(1967) found that for bleed coefficients (base bleed speed/freestream speed) greater than 0·15 the steady value of the base pressure was reached and that for coefficients greater than 0·095 the formation region was extended. The effect of splitter plates in the wake with a gap between the plate and the cylinder has been investigated by many workers. Some eight workers, shown in Table 1, have found a critical gap size below which shedding from circular cylinders is suppressed. The mean critical gap size was $5{\cdot}1 \pm 0{\cdot}3$ radii.

Strykowski & Sreenivasan (1985) reported on a series of intriguing results. They found that vortex shedding can be suppressed at least over a limited range of Reynolds number by the advantageous positioning in the near wake of a second much smaller cylinder parallel to the first. Suppression was achieved in the range $40 < \mathrm{Re} < 80$ when the control cylinder or rod is in the shear layer bounding the near wake. Mildly heating the control rod with direct current considerably widens the range of positions in the wake which produce steady flow and the area increases with increased heating. Heating is more effective when the rod is in the shear layer but also functions with the rod on the wake axis. With the unheated rod they observed that flow is diverted into the near wake region by the control rod. Not unexpectedly the whole character of the instability of the near wake is thus changed but only for restricted positions. In an extended account Strykowski & Sreenivasan (1990) found that the control is effective also in the wakes of cylinder shapes with fixed separation points and that two symmetrically placed control rods are more effective than one. Their results of a numerical analysis show that the control rod in the shear layer spreads the velocity gradient, reducing maximum vorticity. They suggest that the flow stability is directly related to the maximum vorticity in the shear layers, but other factors such as freestream disturbance level and body vibration also determine the critical Re. Beyond the range in which the shedding is suppressed, the control rod reduces the shedding frequency. Spectra were measured at 50 diameters downstream with the shedding suppressed by placing the

control rod in its optimum position. These show peaks in the spectrum at a somewhat lower frequency than the natural shedding frequency, and at the higher Re these are accompanied by their first harmonic. This seems to support their contention that the mean velocity distribution is the most significant aspect of the growth of disturbances which is a process essentially independent of the body. They maintain that, in direct contrast to the experiments we report here, the stable wake at $Re < Re_c$ cannot be made unstable with a control rod in the wake.

Recent applications of stability theory have concentrated on bluff-body wakes, and these are to be found in the publications of Koch (1985), Huerre & Monkewitz (1985), Triantafyllou *et al.* (1986), Monkewitz & Nuygen (1987), Chomaz *et al.* (1988), Monkewitz (1988) and reviewed by Huerre & Monkewitz (1990).

There is now increasing evidence that wake flows exhibit self-sustained oscillations by feedback from the near wake to the body, [Strykowski & Sreenivasan (1990) being one exception to this view]. Monkewitz (1988), used the criterion which requires the behaviour of the temporal growth rate of the dominant discrete mode at the location of the impulsive source. His analysis of the asymptotic response at large time showed that this is determined by the complex group velocity becoming zero and that this corresponds to a square-root branch point of wave number. If the absolute growth rate, w_i at the branch point is positive and the branch point results from the coalescence of an upstream and downstream mode, the instability is absolute. Such absolute instability grows into a limit cycle of oscillation which is the sinuous mode of the Karman vortex street. There is a change from absolute instability in the near wake to convective instability further downstream. Nakaya (1976), Koch (1985) and Chomaz *et al.* (1988) suggested that a resonance builds up, involving wave motions between the body and a reflection site in the wake. The nature of this site of instability in the wake, which involves waves travelling in both directions, is the current preoccupation.

Koch (1985) proposed that the source in the wake is the region where the separated boundary layers surrounding the closed wake-bubble interact at the end of the bubble. Monkewitz (1988) showed that prior to the onset of the global instability, which results in the vortex shedding, there is (at lower Re) a region of absolute instability in the near wake. This, he shows, probably first occurs where the reversed flow is a maximum. As Re increases this region grows in size until it encompasses the generation site at the region of interaction at the end of the bubble. Monkewitz (1988) determines the Reynolds numbers of these transitions, which are in reasonable agreement with observations.

In wind tunnels with low turbulence levels the critical Reynolds number, Re_c, for the start of oscillations in the wake is found to be 49 [see for example Provansal *et al.* (1987)]. This value is in agreement with the absolute instability calculations of Jackson (1987) and Monkewitz (1988). Provansal *et al.* (1987) also show from absolute instability theory that the growth rate factor is $(Re\text{-}Re_c)/(10 \times Re)$. This will be shown to concur with the present results at $Re > Re_c$. In towing tanks, uneven towing speed is usually responsible for a reduced value of Re_c of about 35 (Gerrard 1978). Because of the effect of small disturbances which are dependent on the particular experimental arrangement, the determinations of Re_c have produced conflicting results. Plaschko, Berger & Peralta-Fabi (1993) reproduce photographs of Homann (a student of Prandtl) in which gathers, as found by Taneda (1956), are apparent at $Re = 16{\cdot}75$; an asymmetrical near-wake at $Re = 15{\cdot}8$ and a wake with a wavy dye trace along its centreline at $Re = 27{\cdot}4$. Homann's photographs in the book by Prandtl (1952), however, show a perfectly straight dye trace in the wake at $Re = 32$. Whether or not the observations of wake oscillations at these low Reynolds numbers are the result of

artifacts of the particular experiment, it is clear that a numerical study of these flows would be an illuminating exercise.

2. EXPERIMENTS

The experimental observations of Al-Khafaji (1989) show that the Karman vortex street can be produced at low Reynolds number behind a circular cylinder when a small diameter control cylinder is placed, with its axis parallel to the main cylinder, in certain positions in the near wake. The experiments follow closely those of Strykowski & Sreenivasan (1985, 1990), with the important difference that they produced a stable near wake in a range of Re above the critical Reynolds number, Re_c, at which oscillations naturally start. Our experiments were conceived from the entirely opposite motive of encouraging oscillations in a steady wake at $Re < Re_c$. Our original intention was to pulsate a small diameter deformable cylinder placed in the near wake of the main cylinder. In preparation for these experiments the investigations of the effect of placing a rigid cylinder in the wake seemed to be a logical starting point. The Re of 29 was chosen as being well above the point, $Re = 25$, at which from the work of Monkewitz (1988), one might expect a region of absolute instability to exist in the near wake and significantly below the lowest $Re_c = 35$ observed in our towing tank. The Re of 29 is also above the value of 20 at which cylinder oscillations produced an oscillating wake in the experiments of Taneda (1963) and Nishioka & Sato (1978).

A single circular cylinder of 12·7 mm diameter was towed with its axis vertical and projecting through the surface of the water in a towing tank. The tank was 4000 mm long by 750 mm wide and the water depth in all experiments was 381 mm. The aspect ratio of the cylinder was 30 and the blockage ratio 1·7%. There was a constant gap of 1 mm between the cylinder and the bottom of the tank. This arrangement coupled with a clean water surface promotes vortex shedding parallel to the cylinder axis (Slaouti and Gerrard 1981). The tank was insulated and covered to reduce background motions produced by thermal convection. The water temperature variation was less than 0·2°C and observations were made at the beginning of the day. In these conditions the background velocities were of large scale and less than 0·08 mm/s (3·5% of the cylinder speed of 2·3 mm/s). A second run could not be made less than 4 h after the first if these requirements of background motion were to be met. The control rods placed in the near wake were of diameter d_c. In most cases d_c/d was 0·125 where d is the diameter of the main cylinder. Smaller values of d_c were used in one position of the control rod. Obtaining a constant towing speed is very difficult, and it is not certain that the cylinder and control rod did not possess a velocity fluctuation. The more slender control rod may thus have been caused to vibrate.

The method of experimentation was to observe flow visualization produced by dye. In most cases the dye was introduced slowly by injecting a cloud of dye dissolved in water and mixed with a little methanol to make it neutrally buoyant. A short settling time was allowed for the disturbance caused by the injection to subside. The dye occupied a volume just ahead of the stationary cylinder and covered all but the top and bottom 50 mm of the depth. When the run started impulsively from rest by engaging a clutch, dye entered the separation bubble behind the cylinder in the first stages of the motion. In the other method used, dye solution mixed with a minute amount of detergent was allowed to run onto the surface of the water at the front of the cylinder via a hypodermic tube. The method is described in detail by Al-Khafaji & Gerrard (1989). The flows observed on the surface and below it were in agreement. Photographs were taken with a camera mounted on the towing carriage.

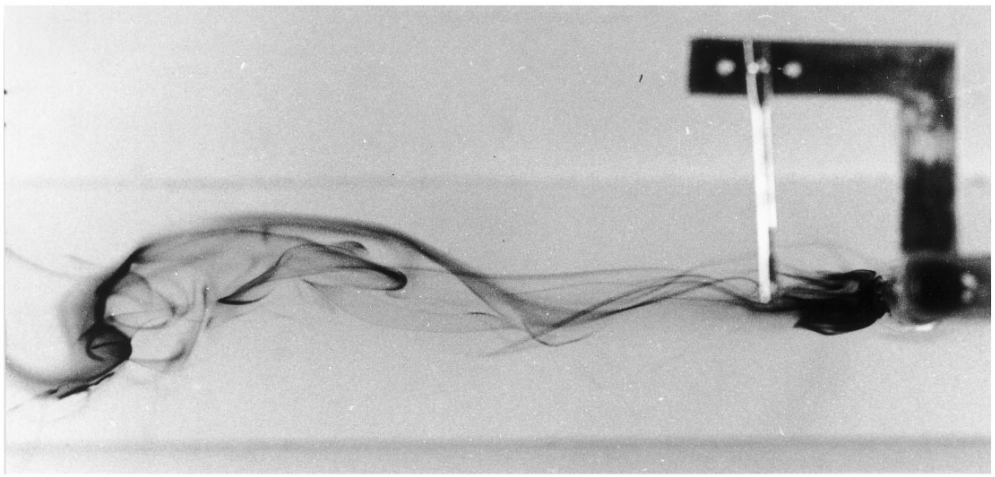

(a)

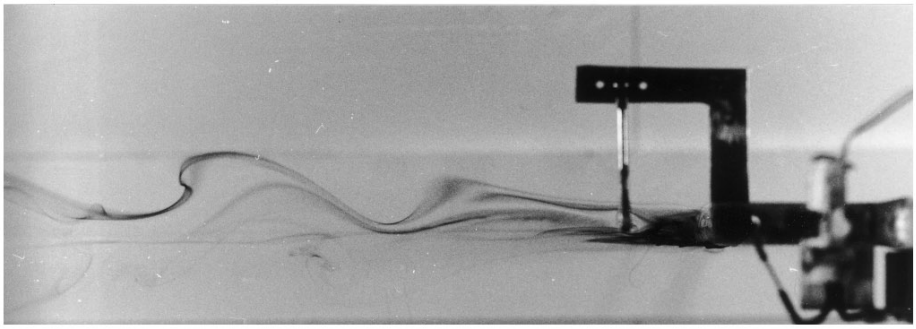

(b)

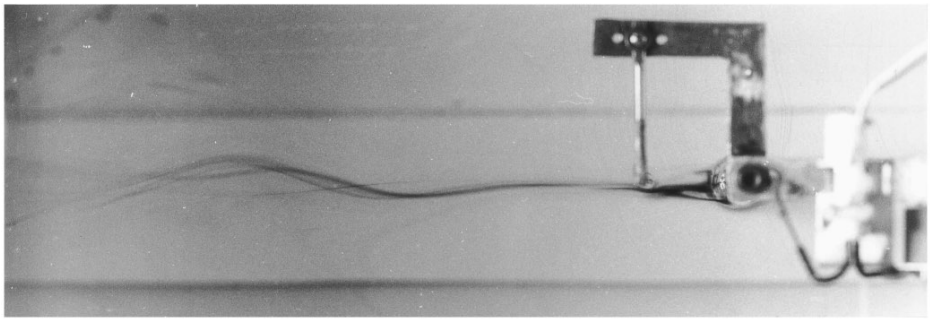

(c)

Figure 1. Flow visualization of the wake oscillations at Re = 29. Control rod at $R = 5$: (a) $d_c/d = 0{\cdot}125$; (b) $d_c/d = 0{\cdot}1$; (c) $d_c/d = 0{\cdot}09$.

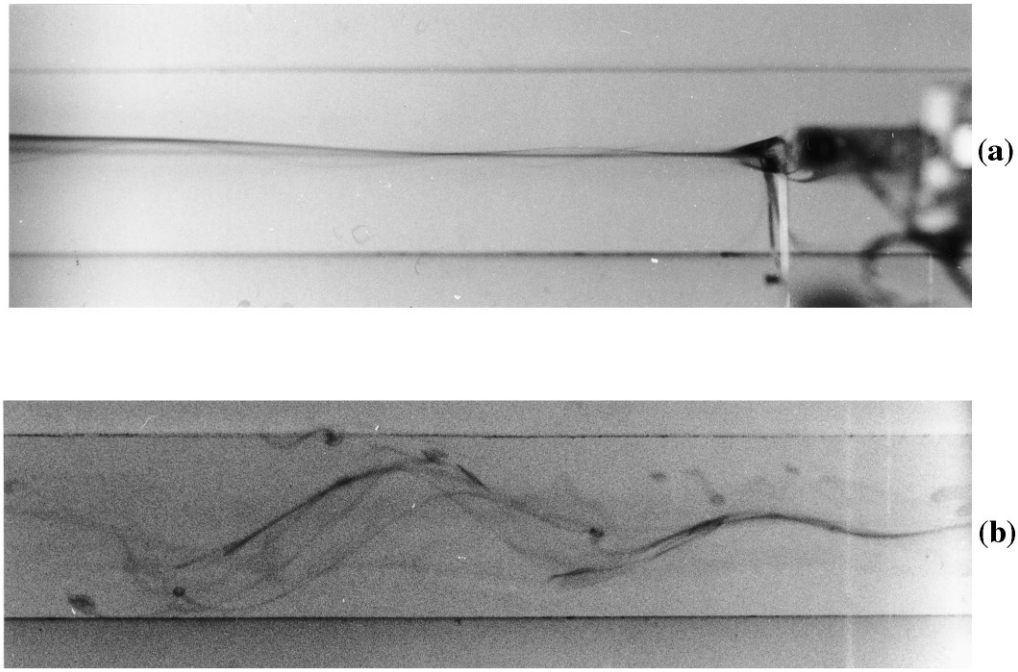

Figure 2. Flow visualization of the wake at Re = 29. Control rod in contact with the rear of the cylinder: (a) the near wake; (b) the wake at $r = 140$.

The range of R of control rod position on the wake axis for which oscillations were observed was found to be 3·6 to 6·25. The definition of the symbols is to be found in the nomenclature in the appendix. Figure 1 clearly shows wake oscillations produced with the control rod on the wake centreline at a gap size of $2{\cdot}0d(x = 5)$. The photograph was taken with dye solution fed onto the water surface in front of the cylinder. Before the photograph was taken the dye flow was switched off by means of a solenoid valve [visible in Figure 1(b, c)]. Large oscillations are clearly seen. The oscillations with the control rod in this position were stronger than those obtained with other positions. At other positions of the control rod on the wake axis, oscillations developed downstream and not at the control position. Figure 1(b, c) shows that the effect of reducing the control rod diameter was to decrease the amplitude of the wake oscillations. With $d_c/d = 0{\cdot}014$ the near wake oscillation disappeared.

In one set of observations which are shown in Figure 2, the control rod ($d_c/d = 0{\cdot}125$) was in contact with the cylinder surface at the rear stagnation point. Flow visualization was achieved by dye washed from the control rod. Dye paste was painted onto a mid-span section and allowed to dry before immersion of the cylinder. The run started after a short settling time during which disturbances subsided. Oscillations were almost absent from the near wake but developed downstream as seen in Figure 2(a, b). The spots of dye seen in Figure 2(b) were due to the accumulation of dye and its fall under gravity.

In the experiments at $\mathrm{Re} = 29$ the control rod positions which produced wake oscillation were on the wake axis only, and only at $R = 1$ and $3{\cdot}6 < R < 6{\cdot}25$. Various positions off the wake axis produced no oscillation even those with $R = 4{\cdot}5$ and 6 but only $0{\cdot}5a$ off the axis.

3. NUMERICAL STUDY

The numerical analysis uses a scheme developed by Benson *et al.* (1989) in which the convection and diffusion terms of the Navier–Stokes equations are separately solved at each time step. Vortices are placed on the cylinder surface to represent a vortex sheet which satisfies the no-slip condition. These vortices are convected with velocities determined from the solution of the convection Poisson equation obtained with a Fast Fourier Transform Poisson Solver library programme (Le Bail 1972). The vortices are then diffused and redistributed, new vortices being formed at the grid intersections due to the spreading in the diffusion time step which is generally twice as long as the convection time step. The convection mesh is a radially exponentially expanding polar mesh. The diffusion and redistribution is performed on an expanding polar mesh in the boundary region (of width equal to one cylinder radius) and also on an overlapping rectangular mesh of fixed spacing. The values of quantities are nondimensionalized with the freestream speed and the cylinder radius. The Re values quoted are based on cylinder diameter. Test programmes used to validate the method and its convergence are included in the paper of Benson *et al.* (1989).

A vortex pair disturbance was used to represent a control rod in the wake. The strength of the two vortices was determined from the velocities at the adjacent mesh points. Their separation represents the size of the body. This is crudely the same process as at the cylinder surface. The control body vortices were inserted at each convective time step and after their introduction they were convected, diffused and redistributed like all the other vortices. The ensuing disturbance to the flow became unstable for a range of positions of the vortex pair and the control vortex pair asymmetry (CVA, the sum of the two vortex strengths) grew exponentially. In all but

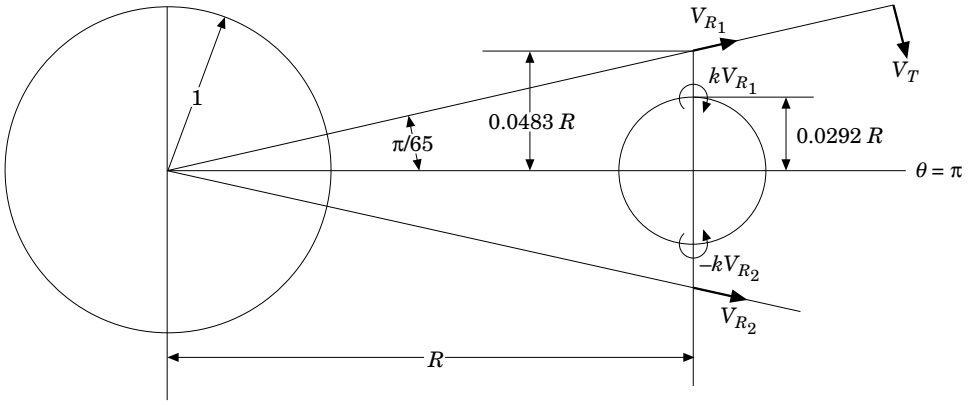

Figure 3. Assignment of control vortices.

one case the vortices were centred on the wake axis. The vortex strength was a factor, k, times the radial velocity at one mesh length from the axis ($k = 0{\cdot}03$, $0{\cdot}04$, $0{\cdot}05$, $0{\cdot}08$ and $0{\cdot}12$). Only one computation with $k = 0{\cdot}12$ was made. The geometry of the control body and the vortices introduced are shown in Figure 3. The control vortex strength, CVS, was determined by the radial velocities V_{R_1} and V_{R_2} which are initially equal since the wake is symmetrical. The control vortices were placed at the positions $\pm 0{\cdot}029R (\approx 0{\cdot}6 \times 0{\cdot}0483)$ and convected downstream; their strength kV_R is equivalent to the semi-circumference of the control body times the mean surface velocity over that half of the body. The presence of vortices produces a wake asymmetry (when $V_{R_1} \neq V_{R_2}$) which grows with time, and oscillations develop. The difference in the strength of the vortices on the two sides of the body produces an induced crossflow velocity at the cylinder. If the vortices from the control body were not convected and diffused, their presence had no effect. Later consideration after the work was completed revealed that this routine produces vortices which are too strong. The vortices were shed from the body at full strength and this neglects the weakening by interaction in a formation region. It is not clear that a better model could be produced simply by reducing k.

The work of Coutanceau & Bouard (1977) on the unsteady flow past a circular cylinder started from rest, has important applications to the present work. In these flows at low Re the bubble-like symmetrical recirculating region behind the body grows in length with time T. At $\mathrm{Re} = 31$ they quote growth from $L = 0$ at $T = 0$ to $1{\cdot}4$ at $T = 4$, $2{\cdot}5$ at $T = 8$ and to its final position of $3{\cdot}1$ at $T \geq 16$. Their closed wake shape at $\mathrm{Re} = 30$ is plotted in Figure 4 which also shows the points at which the near-wake velocity asymmetry was determined in the present work. The velocity asymmetry is the difference between tangential velocity values symmetrically disposed about the wake centreline and when on the axis, is the value of $V_T : V_T$ is shown on Figure 3. Beyond the closed wake the velocity on the axis decreases with distance down the wake. The published curves (Coutanceau & Bouard 1977) are linear down to $0{\cdot}2U$ where the measurements end. Extrapolating the lines to zero velocity has the following result: $u = 0$ at $r = 5$ at $T = 4{\cdot}4$, $r = 8$ at $T = 7{\cdot}6$, $r = 12{\cdot}5$ at $T = 14{\cdot}4$ and $r = 17$ at $T = 21$. This is a linear variation. As a result of this the velocity on which CVS is based increases with time at a fixed R and at large R the growth of CVS is delayed.

4. RESULTS AT A REYNOLDS NUMBER OF 29

The computation was made on the Amadahl 5890 of the Manchester Computing Centre. The central processor time used for runs up to $T = 60$ was about 2000 s. The

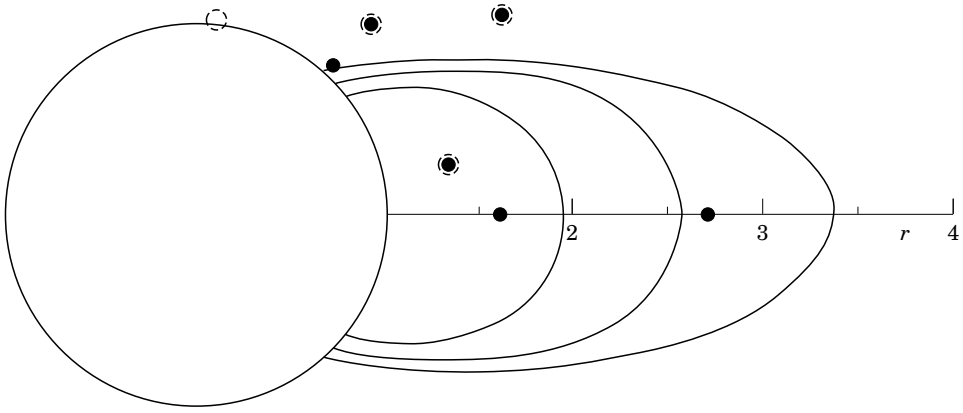

Figure 4. Evolution of the closed wake shape at Re = 30 from Coutanceau & Bouard (1977) at times $T = 2{\cdot}4$, $4{\cdot}8$ and $12{\cdot}6$. The points show positions at which velocity asymmetry was determined: ○, for Figure 9; ●, for Table 2.

development of the flows was monitored by determination of the lift and drag coefficients, C_L and C_D, of the cylinder, the velocity asymmetry at pairs of points equidistant from the wake axis, the control vortex pair asymmetry, CVA, and the vorticity on the wake axis.

Leaving aside the vorticity development for the moment, Figures 5 to 9 show the time variation of the other quantities for the control on the wake axis at $R = 5$ and $k = 0{\cdot}04$. Figure 5 shows the exponentially growing C_L (full line) which only reaches a small amplitude by $T = 60$. Also shown is the C_L obtained with no control in the wake. The variation of the control asymmetry, shown in Figure 6, is much smoother and this was always the case. The strength of one of the control vortices CVS is shown in Figure 7. The magnitude of the strength decreases as the flow developed because the radial velocity decreases with time. Radial and tangential velocities refer to directions on the polar mesh centred on the main cylinder as shown in Figure 3. Initially the

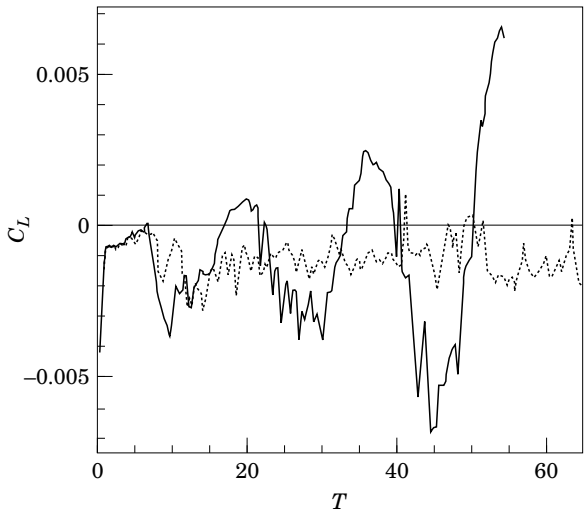

Figure 5. C_L development for $k = 0{\cdot}04$ and $R = 5{\cdot}0$. Broken curve: $k = 0$.

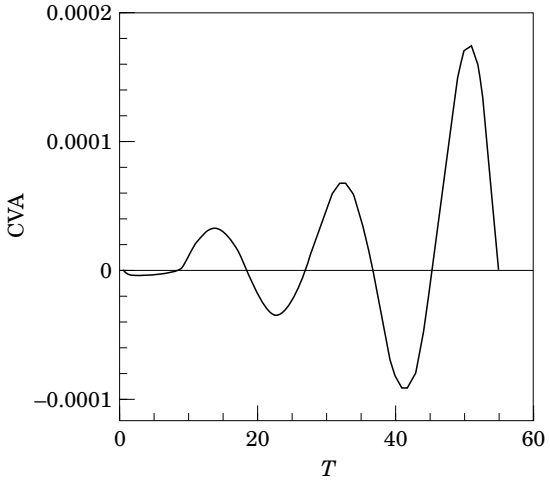

Figure 6. Control vortex asymmetry for $k = 0{\cdot}04$ and $R = 5{\cdot}0$.

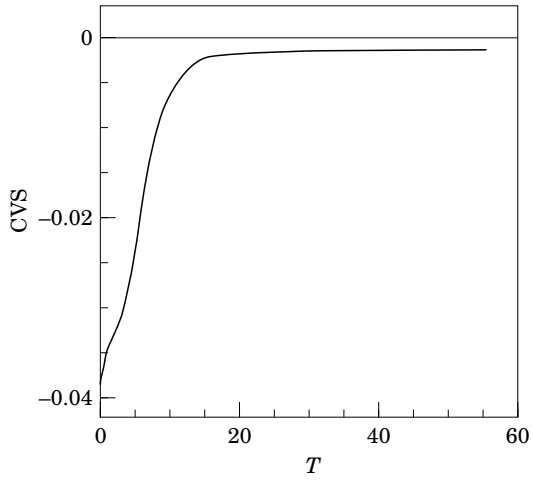

Figure 7. Control vortex strength for $k = 0{\cdot}04$ and $R = 5{\cdot}0$.

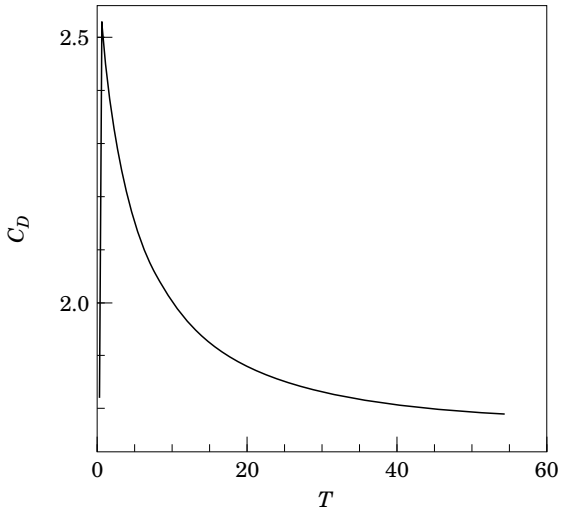

Figure 8. C_D development for $k = 0{\cdot}04$ and $R = 5{\cdot}0$.

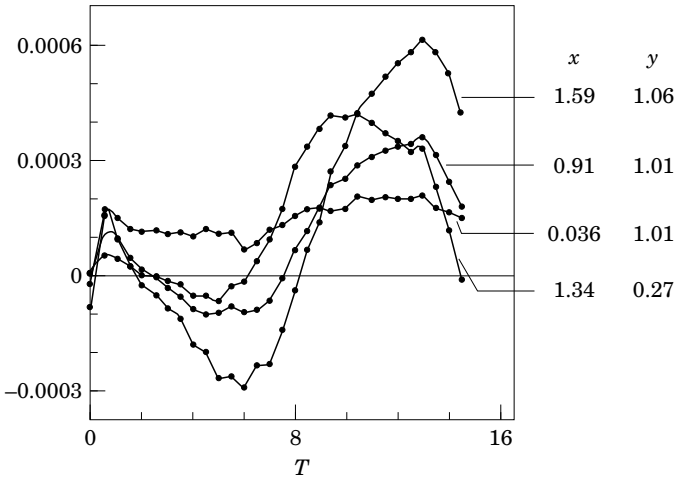

Figure 9. Near-wake velocity asymmetry for $k = 0{\cdot}04$ and $R = 5{\cdot}0$.

control position is outside the bubble-like recirculating region behind the cylinder. This bubble grows with time and if $R < 4{\cdot}65$ the control vortices change sign (to become positive in Figure 7) when the end of the bubble passes the control position. In the time shown C_D has not reached its final level as seen in Figure 8. The difference in circumferential velocity of four pairs of points symmetrically placed with respect to the wake axis is shown in Figure 9. This also grows exponentially. The phase difference between the quantities so far presented is significant and will be discussed. In all cases investigated the Strouhal number was between 0·10 and 0·13, which is higher than the value 0·067 extrapolated from naturally oscillating wakes. In the experiment at $\mathrm{Re} = 29$, the Strouhal numbers of 0·06 and 0·12 were observed. It is possible that the lower value of the Strouhal number is a convective instability which develops downstream.

One case in which the control was off the wake axis was investigated for the conditions $k = 0{\cdot}02$, $R = 5$, $x = 4{\cdot}85$ and $y = 1{\cdot}215$. As might be expected, one sees from Figure 17 that a steady lift is produced. The large initial oscillations slowly decay. The experiments showed no oscillation for this position of the control rod.

4.1. Sequence of the Events Leading to Oscillation

The origin of the growth of disturbances is the aim of the investigation. We look first, therefore, for CVS factors $k = 0{\cdot}04$ and 0·05, at the relative phases of C_L, CVA and the near-wake velocity asymmetry. After the flow starts from rest, the first occurrence, see Figure 9, is the departure from zero of the near-wake velocity asymmetry from zero at $T = 0$. At these early times and at this stage of the development of the work, the oscillations of the near wake were not related to the control vortex asymmetry, which had not yet begun to grow. This is followed by the departure from zero of CVA. The following maxima and minima of CVA lead those of C_L and, as we shall demonstrate, become related to the near-wake velocity asymmetry. At the first maximum of CVA the lead is $4{\cdot}1 \pm 0{\cdot}4$ (r.m.s. deviation of 10 determinations) and at the fourth extremum, $5{\cdot}7 \pm 0{\cdot}4$.

In the later computations in which the numerical noise was much reduced, a clear connection between CVA and the near-wake velocity asymmetry was found.

TABLE 2

Times T_c of the peaks of control vortex asymmetry CVA compared with the mean times T_v of velocity asymmetry at all the points shown in Figure 4. σ_s = r.m.s. deviation of T_v from the mean value

Control k	R									
		T_c	11·7	16·0	23·1	27·2	34·0	39·8	44·4	50·2
0·08	3·43	T_v	11·72	17·14	23·08	28·02	34·29	39·57	45·17	50·78
		σ_s	0·2	0·36	0·42	0·36	0·54	0·47	0·44	0·4
		$\frac{T_c - T_v}{\sigma_s}$	−0·1	−3·2	0	−2·8	−0·5	−0·5	−1·75	−1·45
		T_c					27	33	42	
0·08	5·93	T_v					26·3	33·6	40·0	
		σ_s					0·9	0·9	2·2	
		$\frac{T_c - T_v}{\sigma_s}$					0·8	−0·7	0·9	
		T_c	2·5	9·7	17·1	24·8	35	44	52·7	
0·05	5·93	T_v	2·5	10·2	17·8	25·9	34·1	42·8	51·6	
		σ_s	0·7	1·1	1·0	1·1	1·0	1·1	1·1	
		$\frac{T_c - T_v}{\sigma_s}$	0	−0·4	−0·7	−1·0	0·9	1·1	1·0	

Mean difference = $-0{\cdot}47\sigma_s$

In Table 2 the times, T_c, of the peaks of CVA are compared with T_v, those of the velocity asymmetry at all the points in Figure 4 with the exception of the point at the shoulder of the cylinder. The times T_v varied with distance x downstream. In the range of x in Figure 4, as x increases, T_v rises by dT, falls by the same amount, to rise again also by dT. At the control position $R = 5{\cdot}93$, $\mathrm{d}T \approx 3$ and at $R = 3{\cdot}43$, $dT \approx 1$. Comparison of T_c with the mean values of T_v in Table 2 shows that the peaks are approximately in phase. This supports the idea that when the control takes over, the fundamental driving mechanism is the oscillation at and near the body produced by the velocity field of the control asymmetry. The near wake responds immediately: the lag of C_L is due to change in lift taking time to respond to the velocity field.

Figure 10 shows the positions of the maxima and minima of the wake velocity asymmetry as functions of T for the control absent and present. It is noteworthy that the time development of velocity asymmetry in the wake is similar, whether the control is absent or present; the maxima and minima are delayed without the control. These undulations convect downstream but, with control absent, produce no oscillating lift. The parallel inclined lines correspond to a speed of 0·86, which is the same as the speed of particles from the outer edge of the boundary layer when $T > 3$. These particle paths for control present (outer curve) and absent are shown in Figure 11. We see from Figure 10 that the waves of velocity asymmetry generally convect downstream with the flow. The first maximum with the control present, however, appears all over the near wake region instantaneously when the control is present, but not when it is absent. It was remarked above that the control vortices induce a crossflow at the body. The region of crossflow induction is felt all over the near wake at the same time. The region of instantaneous appearance of the first minimum with control present is much smaller than for the first maximum. The second maximum is entirely convected.

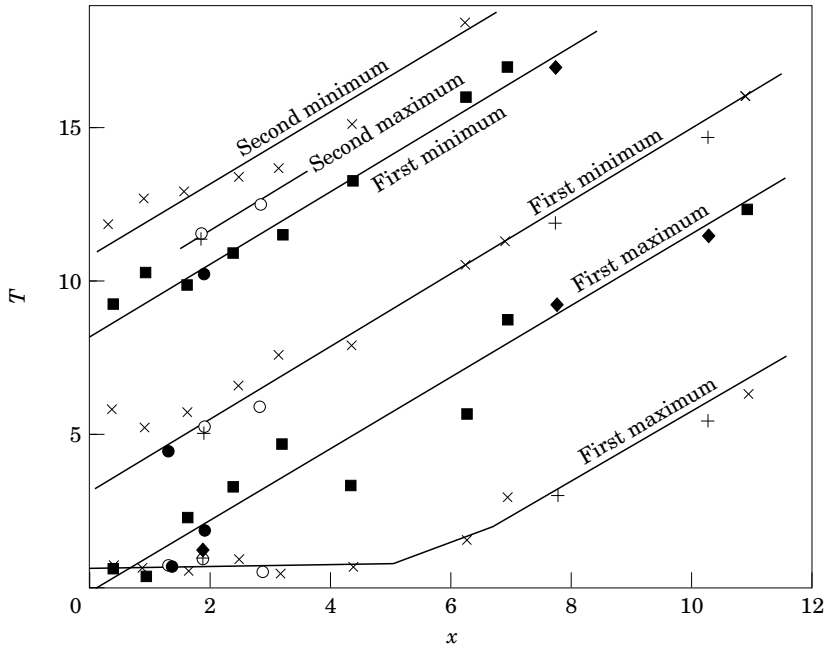

	$k = 0{\cdot}04$	$k = 0$
$y = 1$	×	■
$y = 0{\cdot}27$	○	●
$y = 0$	+	◆

Figure 10. Distance-time relationships of velocity asymmetry maxima and minima. Notation as shown above.

Table 3 shows the phase lead of the velocity asymmetry with respect to C_L. The value of velocity asymmetry departs from zero at time zero whether the control is present or not, when driven by numerical noise. Upstream of the control, the first maximum of the velocity asymmetry at both values of y occurs at approximately the same time before that of C_L. This implies that what happens at the cylinder at this early time is imposed by the whole of the near wake with equal time delay and this delay changes as the instability grows. The bias of C_L to negative values in Figure 5 was dependent on the initial conditions. The results of Figure 5 are presented because the $k = 0$ case was available for these. Later refinements to the access to the Poisson solver produced values of C_L at early times which were very close to zero and smoothly varying, but the $k = 0$ case was not repeated.

The development shown in Figures 5 to 9 was obtained with a single precision computation. At $\mathrm{Re} = 35$ single and double precision was used with $k = 0{\cdot}03$ at $R = 3{\cdot}43$. The variation of the oscillating quantities, C_L, CVA and near-wake velocity asymmetry showed similar trends but were 10^{-10} smaller for double precision, whilst C_D and CVS (the strength of one of the control vortices) were the same. The near-wake velocity asymmetry obtained at all the points shown in Figure 4 exhibited a slight oscillation when $T > 8$ and had larger values at the points further downstream. These results suggest that oscillation starts in the near wake but amplifies when the disturbance reaches the control position, which then feeds back oscillations to the near

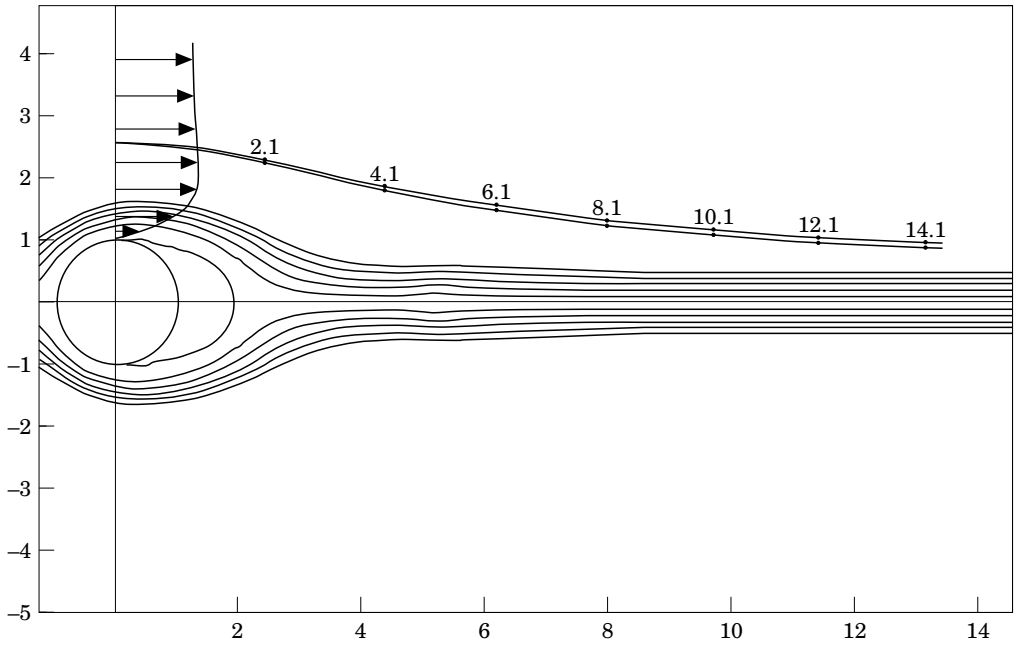

Figure 11. Paths of particles originating from $x = 0$, $y = 2{\cdot}6$ at $T = 0$. Particle positions at later times are shown by the values of T. Streamlines obtained at $T = 2{\cdot}5$. Outer curve is for the control present; inner curve for control absent.

TABLE 3

Times by which the near-wake velocity asymmetry leads C_L at positions x, y. Control vortex $k = 0{\cdot}04$ at $R = 5(x = 5, y = 0)$

Time lead at x	1st maximum	1st minimum	2nd maximum
$y = 1$			
0·4	3·0	5·0	4·5
0·9	3·1	5·5	3·5
1·6	3·0	5·2	3·5
2·5	2·7	4·5	3·1
3·15	3·2	3·3	2·5
4·4	3·0	3·0	1·2
6·28	2·3	0·5	−1·5
$y = 0{\cdot}25$			
1·3	2·5	6·2	6·5
1·9	2·7	5·6	4·8
2·9	3·1	5·0	3·5
4·2	3·0	3·0	1·25
6·2	1·9	0·25	
10·3	−2·8	−4·0	

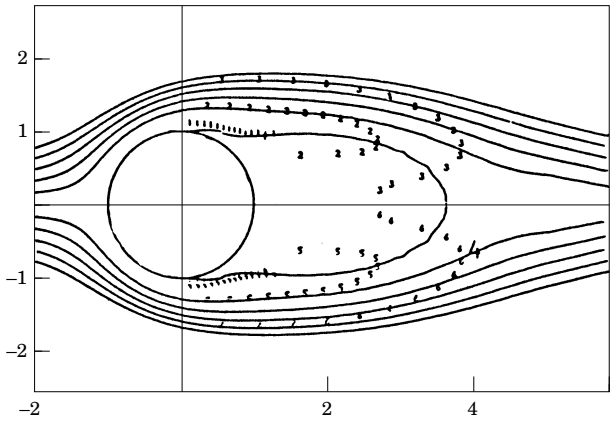

Figure 12. Particle paths from $x = 0$, $T = 0$ and instantaneous streamlines at time $T = 7{\cdot}45$ for $k = 0{\cdot}05$, $R = 5{\cdot}0$.

wake. CVS reached an approximately constant level at $T = 10$: CVA and C_L grew rapidly at $T > 20$.

The vortex strength on the wake axis was determined with the control strength equal to 0·05 at $R = 5$. The background level was the cut-off level of the vortex redistribution which was set at 10^{-5}. The vortex strength on the near wake axis appeared at $T = 7$ for $2{\cdot}5 < r < 5$ and at $T = 10$ had larger values in the range $2 < r < 6$. These times of appearance coincide with the arrival of boundary layer particles in the region of the wake axis inside the region of the wake bubble as shown in Figure 12.

4.2. The Exponential Growth and Decay of Oscillations

The time variation of $\hat{C}_L$ and $\widehat{\text{CVA}}$ during growth and decay were found to be exponential, as Figure 13 shows for $\hat{C}_L$. Figure 14 shows that the values of

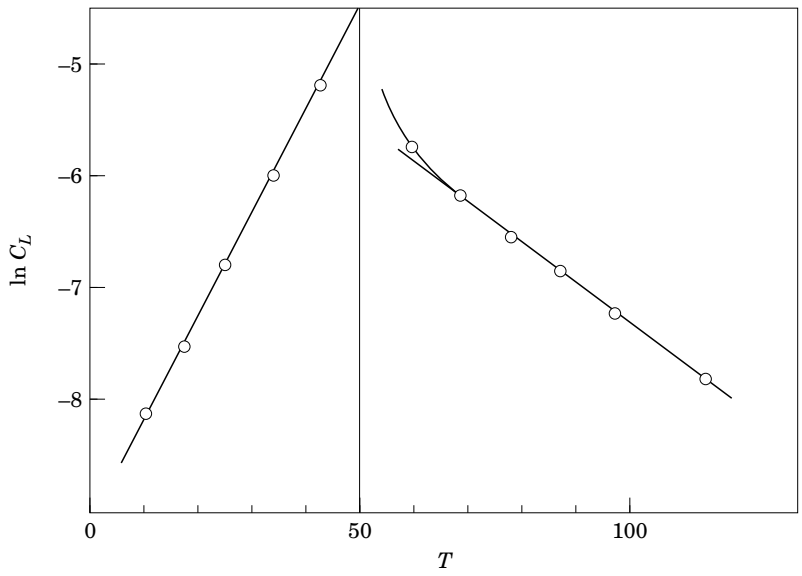

Figure 13. Growth of $\hat{C}_L$ to $T = 50$ with $k = 0{\cdot}03$ at $R = 5{\cdot}0$ and decay with $k = 0$ at $T > 50$.

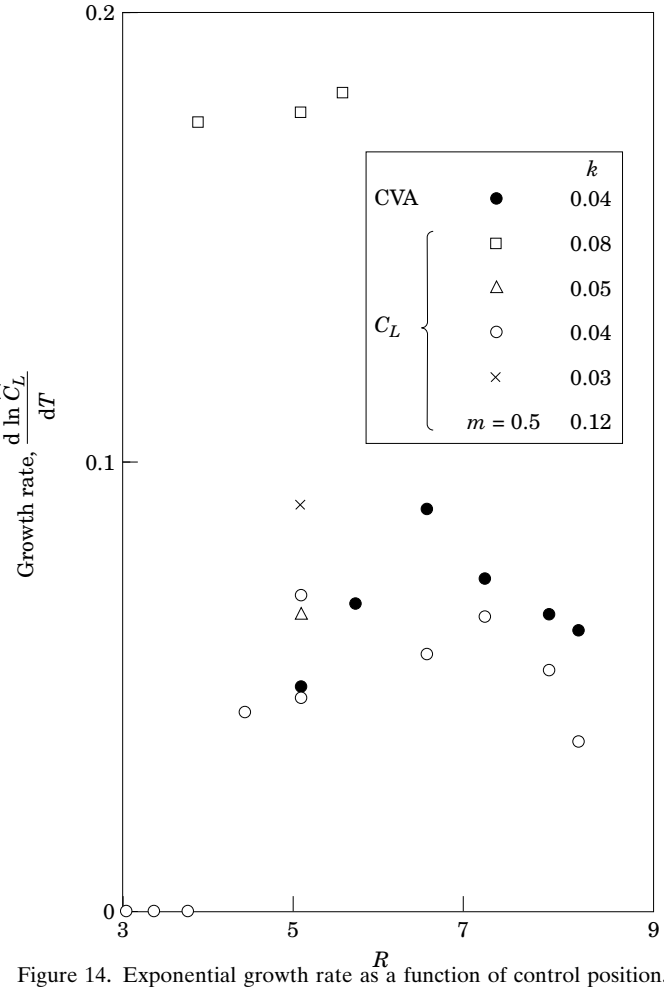

Figure 14. Exponential growth rate as a function of control position.

$m = \mathrm{d} \ln \hat{C}_L/\mathrm{d}T$ and $\mathrm{d} \ln \widehat{\mathrm{CVA}}/\mathrm{d}T$ for these two quantities were essentially the same for the same R and CVS (or k). Most of the results were obtained with $k = 0{\cdot}04$. Oscillations did not grow when $R < 4$ in the time up to $T = 60$. The variation with R of the exponent m has a broad maximum, rising from 0·02 at $R = 4$ to about 0·8 at $R = 6{\cdot}35$ (the critical position below which splitter plates affect the shedding at higher Re is $5{\cdot}1 \pm 0{\cdot}3$); m fell beyond this R to 0·05 at $R = 14$. It was noticed that the start of the exponential rise was delayed in the following cases: to $T = 20$ at $R = 4{\cdot}1$, to $T = 26$ at $R = 5{\cdot}0$, to $T = 38$ at $R = 8{\cdot}1$ and to $T = 29$ at $R = 12{\cdot}6$. This is the behaviour expected from the work of Coutanceau & Bouard (1977) on unsteady wakes. The exponential growth rate was found to increase with k as shown in Figure 15. The approximate relation obtained from this plot is

$$m = 0{\cdot}026 \exp(25k),$$

from which it is seen that the growth rate increases exponentially with k. We see from Table 4 that saturation occurs earlier and the saturation amplitudes increase as k increases. Figure 16 shows exponential growth to saturation corresponding to the first

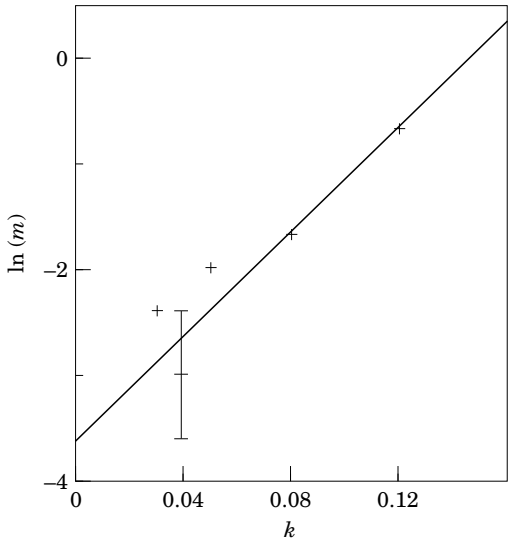

Figure 15. Growth rate as a function of control vortex strength.

TABLE 4
Amplitude growth to saturation

k	R	Time of saturation	Saturation values $\hat{C}_L$	$\widehat{\text{CVA}}$
0·03	5·0	100	0·4	0·01
0·08	3·4	49	0·74	0·045
0·08	4·5	45	1·5	0·05
0·12	4·4	28	2·75	not determined

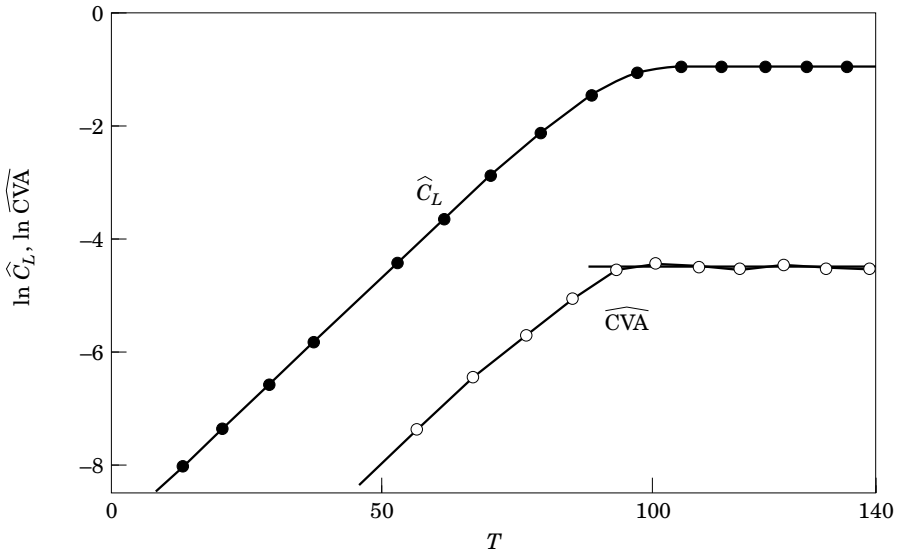

Figure 16. Growth to saturation for $k = 0{\cdot}03$, $R = 5{\cdot}0$.

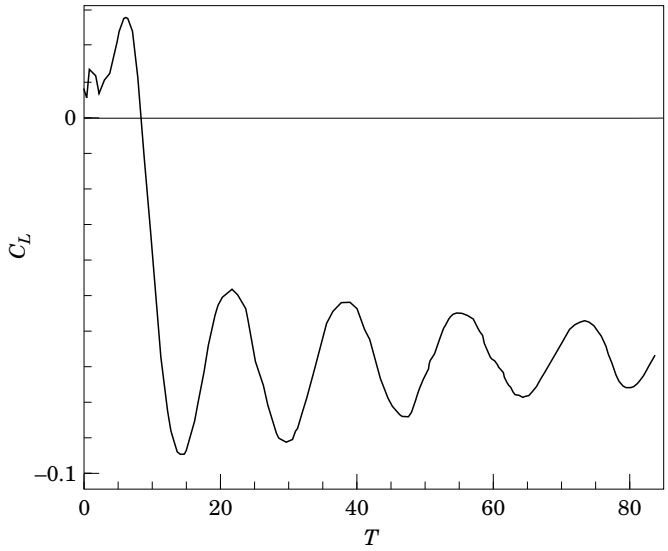

Figure 17. C_L, $k = 0{\cdot}02$ control at $R = 5{\cdot}0$ for $x = 4{\cdot}85$, $y = 1{\cdot}215$.

entry in Table 4. When the control vortex asymmetry has amplified the control vortex strength oscillates also. In the cases of the larger values of $\widehat{\mathrm{CVA}}$ obtained with $k = 0{\cdot}08$ the control vortex strength oscillated also with amplitudes of 0·030 and 0·033. When $k = 0{\cdot}04$ the value of $\hat{C}_L$ at $T = 60$ and $R < 5$ was $1{\cdot}5$ to 3×10^{-3}. At this value of k, $\hat{C}_L$ had a broad maximum of 8×10^{-3} when $R = 8$. This variation of $\hat{C}_L$ with R is similar to the variation of m referred to above and shown in Figure 14. It is at first sight surprising that the control was effective at the position $R = 14$ for which $\hat{C}_L$ was 4×10^{-3}, however the wake is oscillating at this position which produces a strong vortex pair. The control vortices have a velocity field which falls off only inversely with distance.

5. RESULTS OF VARIATION OF REYNOLDS NUMBER

After completion of the work on flows at $\mathrm{Re} = 29$, attention was directed to the analysis of flows for a range of Re. At $\mathrm{Re} \geq 53$, saturation values of $\hat{C}_L$ with no control in the wake resulted from development from the numerical noise or from an initial asymmetry as in Benson *et al.* (1989) up to a Re of 200. These lift coefficients values closely followed the relation

$$\hat{C}_L^2 = 2{\cdot}78 \times 10^{-3}(\mathrm{Re} - 49).$$

This is of the form expected from stability considerations as given, for example, by Schumm *et al.* (1994).

Further work has concentrated on the range $15 \leq \mathrm{Re} \leq 60$. At low Re, growth was followed up to $T = 50$ with $k = 0{\cdot}03$ and $R = 5$: the control was then switched off and the decay followed. At $\mathrm{Re} \geq 45$, growth initiated by numerical noise was studied. At $\mathrm{Re} = 45$ and 53 the waveform was irregular and scarcely left the background level by $T = 115$ and so growth and decay, as at lower Re, was investigated also. At $\mathrm{Re} = 53$,

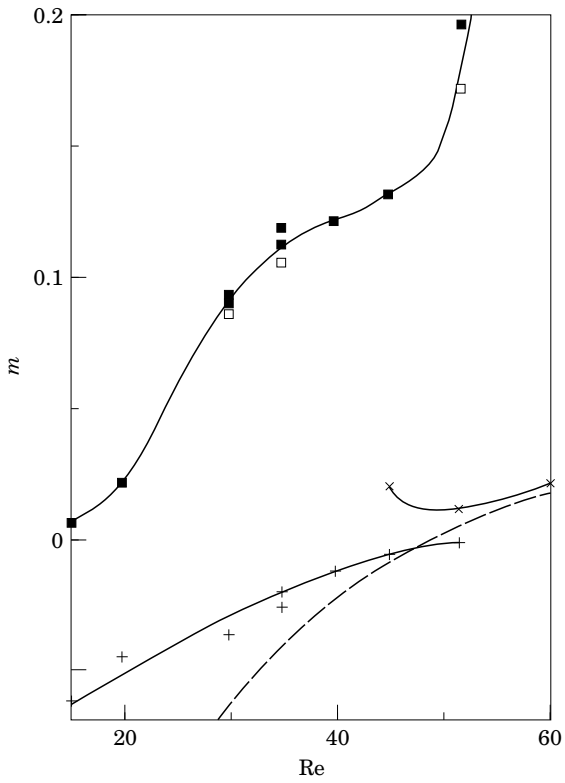

Figure 18. Growth rate as a function of Reynolds number: ■, $\hat{C}_L$ for $k = 0{\cdot}03$, $R = 5{\cdot}0$; □, $\widehat{\text{CVA}}$ for $k = 0{\cdot}03$, $R = 5{\cdot}0$; ×, no control vortices; +, decay at $T > 50$ after growth as in ■; ———, Provansal *et al.* (1987), $\sigma_r = (\text{Re-Re}_c)/10\text{Re}$.

the decay exponent plotted in Figure 18 ended at $T = 120$ and thereafter the amplitude was constant indicating that $\text{Re}_c < 53$. Strouhal numbers, S, are plotted in Figure 19. At all these $\text{Re}(\leq 60)$, the Strouhal number varied during growth and decay. At $\text{Re} > 35$ the final values of S were close to the relationships of Roshko (1954) and Williamson (1988) as seen in Figure 19. During decay, there is only a slight reduction in S at the

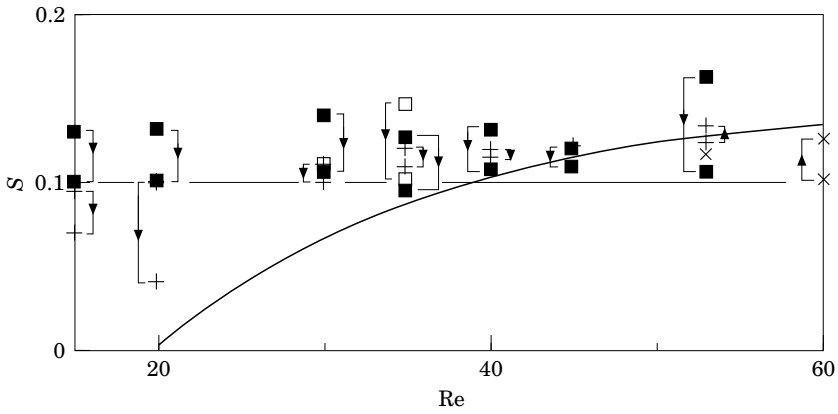

Figure 19. Strouhal number as a function of Reynolds number. Symbols as in Figure 18. —, Universal curve, Roshko (1954) and Williamson (1988) and its extrapolation to $\text{Re} < \text{Re}_c$.

lower Re of 15 and 20 so that the values of S lie above the extrapolation of the curves of Roshko & Williamson.

When there is a control in the wake, the rate of growth exponent m depends on the strength, k, of the control vortices. At higher Re, when the growth is from numerical disturbances, m depends on the magnitude of these. At Re = 15 and 20, m was found to depend on k and R. The growth exponent is plotted in Figure 18 for $k = 0{\cdot}03$ at $R = 5$. The m values show a large reduction only for Re much less than Re_c.

During decay with the control vortices removed for $T > 50$ the exponent m shows fair agreement with σ_r the bifurcation parameter in the Landau truncation of the stability equation determined by Provansal *et al.* (1987) for Re > 40 approximately. The curves in Figure 18 diverge at lower Re.

6. CONCLUSIONS

It had been observed in experiments in a towing tank that it is possible to induce wake oscillations by inserting a control rod on the centreline of the wake of a circular cylinder at Re less than the critical Reynolds number, Re_c, of 35. In a low-turbulence wind tunnel the value of Re_c is found to be 49. A numerical analysis of a model of the same arrangement was therefore initiated at Re = 29. The calculated lift coefficient fluctuated erratically with small amplitude when no control was present in the wake. These fluctuations, due to numerical inexactness, are considered to be the seed of the oscillations found when the vortex pair representing the control body was included in the model. With the control in the wake the lift coefficient amplitude, $\hat{C}_L$, grew exponentially: $\hat{C}_L \propto \exp(mT)$. The growth factor, m, increased with increasing strength, k, of the vortices representing the control body but only when the vortices were shed from the control body and diffused as they were convected downstream. At large values of k, $\hat{C}_L$ values were greater than the spontaneously produced values at high Re. Growth of $\hat{C}_L$ was obtained with a wide range of axial control positions.

The order of growth events in the near wake was analysed. The velocity asymmetry, the difference in flow speed at points at equal but opposite distances from the wake centreline at the same downstream position, was the first occurrence observed. The velocity asymmetry convected downstream, but at $k > 0$ the initial velocity asymmetry appeared over the whole near wake at the same time before, at later times, convecting downstream. Velocity asymmetry was followed by the appearance of asymmetry at the control: the two control vortices became of different strength. The growth of C_L occurred when asymmetric velocities in the near wake were those of the velocity field of the control asymmetry. Most results were obtained with the control vortex strength factor $k = 0{\cdot}04$ and the control positioned at $R = 5$. These results showed that the first maximum of the near-wake velocity asymmetry led that of C_L by $2{\cdot}93 \pm 0{\cdot}02$ and that of CVA led C_L by $4{\cdot}1 \pm 0{\cdot}4$. The region of absolute instability envisaged by Monkewitz (1988) starts at the position of maximum reversed flow at $r = 2{\cdot}3$ (Coutanceau & Bouard 1977) and spreads as Re increases. The phase differences above indicate that, at the low Re considered here, the absolutely unstable region communicates with the control, producing asymmetry there which then affects the flow at the surface of the body and hence C_L. Control vortices at small values of r produced no exponential growth. To test the Monkewitz theory one should strictly introduce the disturbance after the steady flow is established rather than at $T = 0$, but if there has been no effect up to the steady flow establishment time the control presence should start to have an effect as if it was just introduced. In the natural onset of oscillations at higher Re, triggered by small disturbances, Koch (1985) has suggested that the site of

first asymmetry is at or just beyond the end of the wake bubble to where the region of absolute instability has spread.

The effect of variation of Re below and above the Re = 29 value was investigated. At $Re \geq 53$ the growth factor, without control in the wake, was found to have the value $(Re - Re_c)/10\ Re$ (with $Re_c = 49$) as predicted by absolute instability theory (Provansal *et al.* 1987). The Strouhal numbers were in agreement with the well-established experimental variation with Re. At $Re < 29$ the growth rate decreased and during decay ($k = 0,\ T \geq 50$) lay above the curve of Provansal *et al.* The Strouhal numbers remained at values close to 0·1.

In the experiments, there were possibilities of the forcing of oscillations by factors dependent on the particular experimental arrangement. It is possible that there are numerical instabilities which contribute to the behaviour of the numerical results, but double precision computation, though considerably reducing the rate of growth did not inhibit growth. Even though any computing scheme will have numerical noise it would be desirable to model the flow with a different scheme. The first priority for improvement is better modelling of shedding from the control body. The present vortex shedding from the control body is too simplistic. Vortices are shed from the body rather than after interaction in a formation region which results in weaker vortices being shed.

References

Al-Khafaji, A. A. 1989 Instabilities in the near wake of a circular cylinder at low Reynolds number. Ph.D. Thesis, University of Manchester.

Al-Khafaji, A. A. & Gerrard, J. H. 1989 Water surface flow visualisation of bluff body wakes. In *Proceedings 5th International Symposium on flow visualisation* (ed. R. Reznicék). Washington D.C. Hemisphere.

Bearman, P. W. 1967 On vortex street wakes. *Journal of Fluid Mechanics* **28,** 625–641.

Benson, M. G., Bellamy-Knights, P. G., Gerrard, J. H. & Gladwell, I. 1989 A viscous splitting algorithm applied to low Reynolds number flows round a circular cylinder. *Journal of Fluids and Structures* **3,** 439–479.

Chomaz, J. M., Huerre, P. & Redekopp, L. G. 1988 Bifurcations to local and global modes in spatially-developing flows. *Physical Review Letters* **60,** 25–28.

Coutanceau, M. & Bouard, R. 1977 Experimental determination of the main features of the viscous flow in the wake of a circular cylinder in uniform translation; I. Steady flow. *Journal of Fluid Mechanics* **179,** 231–256.

Gerrard, J. H. 1978 The wakes of cylindrical bluff bodies at low Reynolds number. *Philosophical Transactions of the Royal Society* (*London*) **288,** 351–382.

Grove, A. S., Shair, F. H., Petersen. & Acrivos, A. 1964 An experimental investigation of the steady flow past a circular cylinder. *Journal of Fluid Mechanics* **19,** 60–80.

Huerre, P. & Monkewitz, P. A. 1985 Absolute and convective instabilities in free shear layers. *Journal of Fluid Mechanics* **159,** 151–168.

Huerre, P. & Monkewitz, P. A. 1990 Local and global instabilities in spatially developing flows. *Annual Review of Fluid Mechanics* **22,** 473–537.

Ishigai, S., Nishikawa, E., Nishimura, K. & Cho, K. 1972 Experimental study on structure of gas flow in tube banks with tube axes normal to the flow. Part 1. Karman vortex flow around two tubes at various spacings. *Bulletin of the Japan Society of Mechanical Engineers* **15,** 949–956.

Jackson, C. P. 1987 A finite element study of the onset of vortex shedding in flow past variously shaped bodies. *Journal of Fluid Mechanics* 182, 23–45.

Koch, W. 1985 Local instability characteristics and frequency determination of self-excited wake flows. *Journal of Sound and Vibration* 99, 53–83.

Leal, L. G. & Acrivos, A. 1969 The effect of the base bleed on the steady separated flow past bluff objects. *Journal of Fluid Mechanics* 39, 735–752.

LeBail, R. C. 1972 Use of first Fourier transforms for solving partial differential equations in physics. *Journal of Computational Physics* **9,** 440–465.

Monkewitz, P. A. 1988 The absolute and convective instability in two-dimensional wakes at low Reynolds number. *Physics of Fluids* **5,** 999–1006.
Monkewitz, P. A. & Nguyen, L. N. 1987 Absolute Instability in the near wake of two-dimensional bluff bodies. *Journal of Fluids and Structures* **1,** 165–184.
Nakaya, C. 1976 Instability of the near wake behind a circular cylinder. *Journal of the Physical Society of Japan* **41,** 1087–1088.
Nishioka, M. & Sato, H. 1978 Mechanism of determination of the shedding frequency of vortices behind a cylinder at low Reynolds numbers. *Journal of Fluid Mechanics* **89,** 49–60.
Plaschko, P., Berger, E. & Peralta-Fabi, R. 1993 Periodic flow in the near wake of straight circular cylinders. *Physics of Fluids* A **5,** 1718–1724.
Prandtl, L. 1952 *Essentials of Fluid Dynamics.* London: Blackie & Son.
Roshko, A. 1954 On the drag and shedding frequency of two-dimensional bluff bodies. NACA TN 3169.
Provansal, M., Mathis, C. & Boyer, L. 1987 Bénard-von Kármán instability: transient and forced regimes. *Journal of Fluid Mechanics* 182*,* 1–22.
Plaschko, P., Berger, E. & Peralta-Fabi, R. 1993 Periodic flow in the near wake of straight circular cylinders. *Physics of Fluids* A **5,** 1718–1724.
Schumm, M., Berger, E. & Monkewitz, P. A. 1994 Self-excited oscillations in the wake of two-dimensional bluff bodies and their control. *Journal of Fluid Mechanics* **271,** 17–53.
Shair, F. H., Grove, A. S., Petersen, E. E. & Acrivos, A. 1963 The effect of confining walls on stability of the steady wake behind a circular cylinder. *Journal of Fluid Mechanics* **17,** 546–550.
Slaouti, A. & Gerrard, J. H. 1981 Experimental investigation of the end effects on the wake of a circular cylinder towed through water at low Reynolds number. *Journal of Fluid Mechanics* **112,** 297–314.
Strykowski, P. J. & Sreenivasan, K. R. 1985 The control of transitional flows. In *Proceedings A.I.A.A. Shear Flow Control Conference,* Boulder, Colorado. Paper 559, pp. 4–12.
Strykowski, P. J. & Sreenivasan, K. R. 1990 On the formation and suppression of vortex shedding at low Reynolds numbers. *Journal of Fluid Mechanics* **218,** 71–107.
Taneda, S. 1956 Experimental investigation of the wakes behind cylinders and plates at Low Reynolds number. *Journal of the Physical Society of Japan* **11,** 302–307.
Taneda, S. 1963 The stability of two dimensional laminar wake at low Reynolds numbers. *Journal of the Physical Society of Japan* **18,** 288–296.
Thomas, D. G. & Kravs, K. A. 1964 Interaction of vortex sheet. *Journal of Applied Physics* **35,** 3458–3459.
Triantafyllou, G. S., Triantafyllou, M. S. & Chryssostomidis, C. 1986 On the formation of vortex streets behind stationary cylinders. *Journal of Fluid Mechanics* **170,** 461–467.
Unal, M. F. & Rockwell, D. 1988 On vortex formation from a cylinder. Part 1: The initial instability. *Journal of Fluid Mechanics* **190,** 491–512.
Williamson, C. H. K. 1988 Defining a universal and continuous Strouhal-Reynolds number relationship for laminar vortex shedding of a circular cylinder. *Physics of Fluids* **31,** 2742–2744.
Wood, C. J. 1963 The effect of base bleed on a periodic wake. *Journal of the Royal Aeronautical Society* **68,** 477–482.
Zdravkovich, M. M. 1977 Review of flow interference between two circular cylinders in various arrangements. *ASME Journal of Fluids Engineering* **99,** 618–633.
Zdravkovich, M. M. & Stanhope, D. J. 1972 Flow pattern in the gap between two cylinders in tandem. University of Salford Internal Report FM 5/72.

APPENDIX: NOMENCLATURE

a	cylinder radius
d	cylinder diameter
U	free-stream speed

The following are nondimensionalized with U and a:

r	radial coordinate, distance from cylinder centre
x	coordinate along the wake axis
y	coordinate perpendicular to x, origin cylinder centre

R	radial coordinate of control vortex pair
T	time
CVA	control vortex pair asymmetry
	sum of the pair of vortex strengths
CVS	control vortex strength
	$k \times$ radial velocity one mesh length from the wake axis
k	CVS factor

The following are nondimensionalised with U and d;

Re	Reynolds number
Re_c	critical Re for first appearance of naturally occurring oscillating wake
C_L	lift coefficient
C_D	drag coefficient
^	as in $\hat{C}_L$ and $\widehat{\mathrm{CVA}}$ signifies amplitude